Journal of Structural Engineering Vol.43A (March 1997) JSCE

Nominal Strength Size Effect of Brittle Materials Based on Micromechanics

Guo-ping YANG[1] and Hiroshi HIKOSAKA[2]

1) Ph.D., Guest researcher from Tsinghua University, China; Dept. of Civil Eng., Kyushu University, Fukuoka
2) Dr. Eng., Professor, Dept. of Civil Eng., Kyushu University, Hakozaki 6-10-1, Higashi-ku, Fukuoka 812, Japan

Abstract

The nominal strength size effects of brittle materials in both tension and compression are studied in micromechanics framework, considering microcrack interaction, propagation and coalescence in finite sized specimens. Two numerical micromechanics models are proposed to study the coupling between microcracks and finite sized boundary. Adoption of these two models depends on the balance between more realistic curved crack propagation trajectories of only several cracks and simplified straight propagation paths of many microcracks. It is verified that the usual Size Effects with -1/2 slope in bilogarithmic form are only applicable to geometrically similar cases. In geometrically dissimilar cases, however, the size effects present very different features in both tension and compression.

Keywords: Micromechnics, Size effects, Fracture, Brittle materials

1. Introduction

The nominal strength size effect of the brittle materials is a special term to mean the phenomenon that the strength of a structure decreases as the structural size increases. For a long time, it has been explained statistically as the assumption that a weaker material point is more likely to occur in a larger structure. For example, many explanations were based on the Weibull weakest-link theory. In 1984, Bazant connected reasonably the size effect of concrete structure with energy release during the crack propagation[1]. It has been evidenced from extensive experiments that the failure mechanism of brittle materials is dependent on the crack propagation behavior in both tensile and compressive loading conditions. The pre-existing microimperfections in brittle materials play a very important role in nominal strength size effects.

Since the brittle materials is very crack-sensitive, many researchers attributed the macro-mechanical properties of brittle materials to the micro-structures and micro-mechanism of crack behavior[2-4]. Great effort has been made for considering the crack interaction and propagation in brittle materials[5-8]. But there were rarely considerations of finite size boundary influence in previous work, and what is more, the usual size effects are referred to the geometrically similar specimens, which means that the ratio of crack length to specimen size is kept proportional in cracking problems, as the Bazant's hypothesis shown in Fig.1. However, this is rather far from the practical engineering situations where the proportional ratio does not always hold.

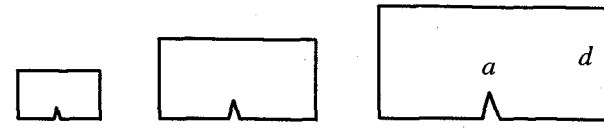

Fig.1 Bazant's hypothesis (a/d=constant).

In real situations, strength size effect is closely connected with the coupling between crack behavior and the finite sized boundary influences. Although many studies have been done for geometrically similar cases, the fracture characteristics and the strength size effects are not completely understood in the complicated case where geometrical dissimilarity exists.

In the present paper, the nominal strength size effects of brittle materials in tension and compression are studied in the micromechanics framework, considering the microcrack interaction, propagation and coalescence in finite sized specimens with both geometrically similar and dissimilar cases. Two numerical micromechanics models are proposed to study the coupling between microcracks behavior and finite sized boundary influence. In the first model, several microcracks are simulated with the displacement discontinuities boundary elements with more realistic curved propagation trajectories; while in the second model the behavior of a large number of microcracks is represented by the closed form solutions

with simplified propagation paths. The coefficients of crack interaction and boundary influence are obtained in the unified form of algebraic expressions. Realistic curved or simplified straight branching cracks are simulated through a step by step propagation increment. With different configurations of specimen sizes and crack lengths, the influences of specimen size and crack length on the fracture strength of the brittle materials in both tensile and compressive cases are studied. It is shown from the results that the usual Size Effects with -1/2 slope in bilogarithmic form are only applicable to the geometrically similar cases, while in the case geometrical similarity does not hold, size effects take very different mechanical features. The results explain reasonably why the size effects prevail in the brittle materials containing many initial imperfections.

2. Brief Description of the Micromechanics Models

To simulate the microcrack behavior, the crack representation should be properly considered. The choice depends on the number of cracks to be simulated in the specimen. In the case of only several cracks, displacement discontinuity elements are adopted to trace the more realistic curved crack propagating paths, the degrees of freedom increase with the progressive cracking process. When a large number of cracks are to be simulated, the classical closed form crack solutions are used to simplify the cracking trajectories as straight approximations. As for the finite sized boundary, it is suitably represented with the Fictitious Stress elements.

2.1 Displacement Discontinuity Crack Representation

In geometrical terms, cracks are considered to be discontinuities in an extending field. The Displacement Discontinuity Method (DDM) is based on the assumption that stress and displacement fields are connected with displacement discontinuity (DD) over the crack's two surfaces. Based on the analytical solution of a displacement discontinuity in elastic field, a crack is subdivided into a number of DD elements. The resultant field summing up all elements' contributions gives out numerical solution satisfying the given boundary conditions. By subdividing each crack into M number of DD elements, the elemental DDs are defined with respect to local tangential and normal coordinates s and n as D_s and D_n. The stress and displacement fields in local coordinates will be obtained from the contributions of these local DD elements[9]:

$$\sigma_s(i) = \sum_{j=1}^{M} A_{ss}(i,j)D_s(j) + \sum_{j=1}^{M} A_{sn}(i,j)D_n(j) \qquad (1a)$$

$$\sigma_n(i) = \sum_{j=1}^{M} A_{ns}(i,j)D_s(j) + \sum_{j=1}^{M} A_{nn}(i,j)D_n(j) \qquad (1b)$$

$$u_s(i) = \sum_{j=1}^{M} B_{ss}(i,j)D_s(j) + \sum_{j=1}^{M} B_{sn}(i,j)D_n(j) \qquad (1c)$$

$$u_n(i) = \sum_{j=1}^{M} B_{ns}(i,j)D_s(j) + \sum_{j=1}^{M} B_{nn}(i,j)D_n(j) \qquad (1d)$$

in which $A_{ss}(i,j)$, $A_{sn}(i,j)$, $B_{ss}(i,j)$, $B_{sn}(i,j)$, etc. are the influence coefficients of stresses or displacements at location j on those at location i, then the simple coordinate transformation will give out the global effects of these local discontinuities. In the case of several microcracks in specimen, above equations also give out the mutual influences between different cracks.

2.2 Crack Representation with Closed Form Crack Solutions

If many pre-existing microcracks are to be considered, it is convenient to adopt the fictitious stress concept for the computation of the Stress Intensity Factors (SIFs) with interacting cracks. The fictitious stresses are assumed as the on-site stresses acting on the microcrack surfaces and producing the same SIFs as those from remote boundary stresses. For the stress distribution around a crack whose surfaces are subjected to constant normal and shear stresses, Sneddon and Lowengrub obtained closed form solutions[10]. These exact solutions have been used to simulate the interacting microcracks[8,11-12].

Two algorithms are herein adopted for computing the SIFs of interacting microcracks with and without propagation, respectively. The exact solutions from Sneddon and Lowengrub are used for primitive microcracks (not propagated), which allows us to get better estimations for the crack propagation initiation and branching directions, each crack has two degrees of freedom. After the crack has propagated, the approximate K-dominant stress field, commonly used in classical fracture mechanics, is adopted for the computation of the stresses generated by the branching crack tips, six degrees of freedom are adopted to model the crack branching states.

If the primitive crack has propagated with two branching cracks, as shown in Fig.2:

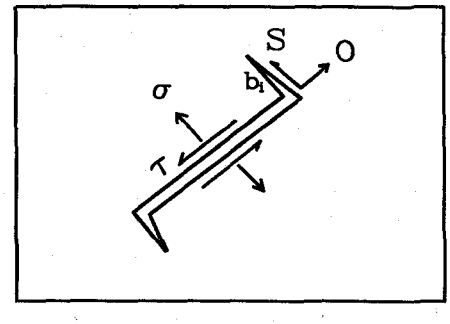

Fig.2 Primitive Crack with two branching tips.

the fictitious stresses σ and τ on the surfaces of the primitive crack, generated by the applied boundary stresses and crack interaction, will result in an opening force O and a sliding force S on the branching cracks[6]:

$$O=\begin{cases} a_i(-\tau sin\theta_{ij}+\sigma\cos\theta_{ij}) & , \quad for \quad \sigma>0 \\ a_i(-\tau sin\theta_{ij}+\sigma\lambda|sin\theta_{ij}|) & , \quad for \quad \sigma<0 \end{cases} \tag{2a}$$

$$S=a_i(\tau+\sigma\lambda)\cos\theta_{ij} \tag{2b}$$

where λ is the friction coefficient between the two crack surfaces in compression. When the normal stress is tensile, the frictional term in the preceding equations is absent.

The SIFs at the crack tips are evaluated from

$$K_I=\frac{O}{\sqrt{\pi b_i}}+\sigma_n\sqrt{\pi b_i} \tag{3a}$$

$$K_{II}=\frac{S}{\sqrt{\pi b_i}}+\sigma_t\sqrt{\pi b_i} \tag{3b}$$

where b_i is the length of the branching crack, σ_n and σ_t are the fictitious normal and shearing stresses on b_i.

If σ_n is tensile, the propagation length b_i should be determined from

$$\frac{a_i(-\tau sin\theta_{ij}+\sigma\cos\theta_{ij})}{\sqrt{\pi b_i}}+\sigma_n\sqrt{\pi b_i}=K_{IC} \tag{4}$$

If the major stress is compressive, the fictitious normal stress on primitive crack is negative in most cases,

$$S=\begin{cases} a_i(\tau+\sigma\lambda)\cos\theta_{ij} & , \quad for \quad \tau>0 \\ a_i(\tau-\sigma\lambda)\cos\theta_{ij} & , \quad for \quad \tau<0 \end{cases} \tag{5a}$$

$$O=a_i(-\tau sin\theta_{ij}+\sigma\lambda|sin\theta_{ij}|) \tag{5b}$$

If the fictitious normal stress on branching crack is also negative, then from

$$\frac{a_i(-\tau sin\theta_{ij}+\sigma|sin\theta_{ij}|)}{\sqrt{\pi b_i}}=K_{IC} \tag{6}$$

it can be seen that the propagation of the branching crack is stable, so the length of the branching crack can be obtained step by step with the increase of the applied external stresses on the specimen.

In the case of M microcracks in the specimen, the interaction between cracks can be determined from

$$\sigma_i=-\sigma_i^{bound}-\sum_{k\neq i}^{M}\left[R_{ik}^{\sigma\sigma}\cdot\sigma_k+R_{ik}^{\sigma\tau}\cdot\tau_k\right] \tag{7a}$$

$$\tau_i=-\tau_i^{bound}-\sum_{k\neq i}^{M}\left[R_{ik}^{\tau\sigma}\cdot\sigma_k+R_{ik}^{\tau\tau}\cdot\tau_k\right] \tag{7b}$$

where σ_i , τ_i are the fictitious normal and shear stresses on crack i, $R_{ik}^{\sigma\sigma}, R_{ik}^{\sigma\tau}$ ... are influence coefficients representing the interaction of crack k on crack i. Eqs.(7) represent $2M$ linear relations for solving $2M$ unknown fictitious stresses, it will be extended to $6M$ to represent the different crack configurations during propagating process.

2.3 Finite Sized Specimen with Interacting Cracks

To take account of the influence of finite sized boundary, the Fictitious Stress Method (FSM) is introduced. FSM is based on the exact solution of a point force acting on an infinite plane[9]. A fictitious stress is assumed to act on the discrete boundary element, which is called Stress Discontinuity (SD) since there exists a stress jump on both sides of the element. Over each element, the stress discontinuity is assumed to vary according to a given mode (constant, linear, etc.), the normal and shear stresses generated by N discrete SD elements are

$$\sigma_s(i)=\sum_{j=1}^{N}C_{ss}(i,j)p_s(j)+\sum_{j=1}^{N}C_{sn}(i,j)p_n(j) \tag{8a}$$

$$\sigma_n(i)=\sum_{j=1}^{N}C_{ns}(i,j)p_s(j)+\sum_{j=1}^{N}C_{nn}(i,j)p_n(j) \tag{8b}$$

where $p_s(j)$ and $p_n(j)$ are the unknown normal and tangential Stress Discontinuities at the mid-point of the boundary elements, $C_{ss}(i,j)$, $C_{sn}(i,j)$, etc. are the influence coefficients of stresses at point j on those at point i.

The FSM formulation is very similar to the former formulations in subsections 2.1 and 2.2, so it can be combined with the former procedures. In the case DD element is used, the external boundary may be divided into N Stress Discontinuity elements as shown in Fig.3, which, with M internal DD elements representing the inner cracks, provides the following $2N+2M$ algebraic equations[12-13]:

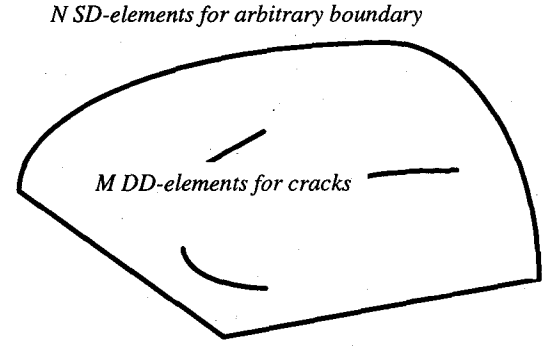

Fig.3 Boundary and crack representation.

$$\sigma_s(i)=\sum_{j=1}^{N}C_{ss}(i,j)p_s(j)+\sum_{j=1}^{N}C_{sn}(i,j)p_n(j)+$$
$$+\sum_{j=1}^{M}A_{ss}(i,j)D_s(j)+\sum_{j=1}^{M}A_{sn}(i,j)D_n(j) \tag{9a}$$

$$\sigma_n(i)=\sum_{j=1}^{N}C_{ns}(i,j)p_s(j)+\sum_{j=1}^{N}C_{nn}(i,j)p_n(j)+$$
$$+\sum_{j=1}^{M}A_{sn}(i,j)D_{sn}(j)+\sum_{j=1}^{M}A_{nn}(i,j)D_n(j) \qquad (9b)$$

In the case many random cracks present in a finite sized body and the closed form crack solutions are adopted, the external boundary can be divided into N Stress Discontinuity elements. These N elements, together with M internal microcracks, give out the following $2N+6M$ algebraic equations to solve the coupling effects:

$$\sigma_i=-\sum_{j=1}^{N}\left[C_{ij}^{pp}pj+C_{ij}^{ps}sj\right]-\sum_{k\neq i}^{M}\sum_{l=1}^{3}\left[R_{ikl}^{\sigma\sigma}\cdot\sigma_{kl}+R_{ikl}^{\sigma\tau}\cdot\tau_{kl}\right] \qquad (10a)$$

$$\tau_i=-\sum_{j=1}^{N}\left[C_{ij}^{sp}pj+C_{ij}^{ss}sj\right]-\sum_{k\neq i}^{M}\sum_{l=1}^{3}\left[R_{ikl}^{\tau\sigma}\cdot\sigma_{kl}+R_{ikl}^{\tau\tau}\cdot\tau_{kl}\right] \qquad (10b)$$

which enables us to determine $2N$ Stress Discontinuity unknowns and $6M$ fictitious stresses for M microcracks.

After getting the stress and displacement fields near the crack tips, the related SIFs can be evaluated considering different propagation configurations in finite sized specimen.

It is necessary to set up the criterion for checking the intersection locations and global failure of the specimen. During crack propagation, some branching cracks may intersect with other cracks, and some minor cracks will stop propagating (Crack Arrest). A coalescence matrix is adopted to identify the independent coalescence clusters[14]. If an independent crack coalescence cluster intersects with two terminal boundary elements, the specimen is assumed at its ultimate load state.

3. Size Effects of Brittle Materials

To the authors' knowledge, almost all previous work concerned with size effects of brittle materials dealt with geometrically similar specimen. In cracking problems, the assumption of geometrically similar specimen means the same ratio of the crack to specimen scaling if only several major cracks presented, as shown in Fig.1. In this case the crack length effect and specimen size effect are the same since the scalings of the crack and specimen are kept proportional. But how about the size effects in the cases without geometrical similarity ? This is specious if the conclusion is simply drawn from the SIFs computations of the classical fracture mechanics.

In the classical Griffith fracture theory in an infinite plate, the crack starts propagating immediately when the SIFs achieve the fracture toughness of the material. The propagation is assumed unstable so the failure stress and crack length were usually connected through the stress singularity of -1/2 in the bilogarithmic form (from $\sigma = K_{I,II}(\pi a)^{-1/2}$). However, when the problem is finite sized and the crack length and specimen size are not exactly geometrically similar, the relation between failure stress and crack length presents different characteristics.

The strength size effects in the geometrically similar cases with several major cracks and many randomly distributed cracks, and the geometrically dissimilar cases of fixed specimen size containing varying crack lengths are studied in the following subsections.

3.1 Geometrically Similar Case with Many Random Microcracks

The crack density and the possible maximum crack size are the most important microstructure parameters of crack distribution in brittle materials. Taking concrete as example, the crack density is connected with many factors such as the cement type, mixture properties, process method and so on. The possible maximum crack size, on the other hand, is usually determined by the maximum aggregate size.

The first group of examples studied in this paper are geometrically similar with many randomly distributed microcracks. This is realized by the equal crack density assumptions in different sized specimens, while the possible maximum crack size is kept the same considering the real situations. Four different sized specimens are computed. The square specimen sides are 50 *mm*, 75 *mm*, 100 *mm* and 150 *mm*, respectively. The material parameters are assumed as: Young's modulus E=30000 N/mm^2, Poisson's ratio ν=03, Fracture Toughness K_{IC}= 20 $N/mm^{3/2}$. Independent uniform distributions for the position and orientation of microcracks in the specimen are adopted. It should be noted that the different combinations of crack position and orientation will give out different internal microstructures. In the examples, 10 samples for each combination of position and orientation are computed, and the average loads are used as characteristic values for size effects.

To keep the crack density unchanged, the numbers of the randomly distributed microcracks are taken as 20, 45, 80 and 180, respectively, for these four different specimen sizes. The possible maximum crack size is assumed to be 5 *mm* in each case.

The crack sizes are assumed with uniform distribution within the range between 0 and 5 *mm*. The average failure loads in uniaxial tension are 4.550 N/mm^2, 3.150 N/mm^2, 2.800 N/mm^2 and 2.625 N/mm^2, respectively. The primitive crack distribution in the 100 *mm* specimen is shown in Fig.4(a), and the crack pattern at failure stage is shown in Fig.4(b). The linear regression relation in bilogarithmic form is

$$Log(\sigma)=3.372-0.495Log(s) \qquad (11)$$

in which σ is the failure stress (in N/mm^2), and s is the specimen side (in *mm*). The slope is very near the strength size effect of -1/2 in the ideal brittle materials from classical linear fracture mechanics.

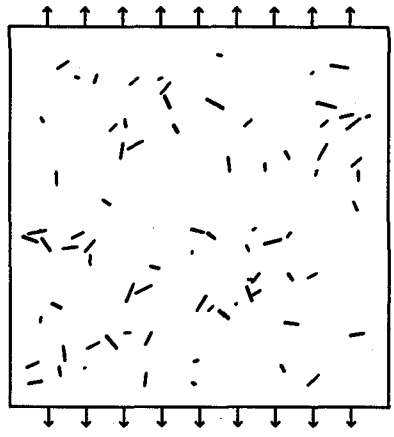

(a) Primitive crack distribution
(Uniform Crack Size Distribution)

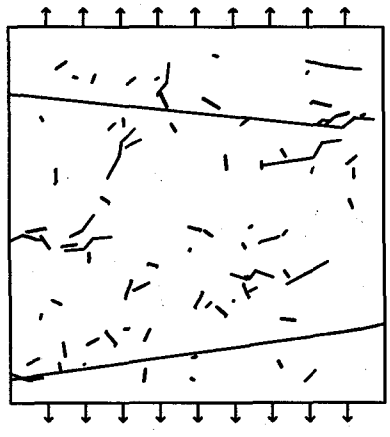

(b) Crack pattern at failure

Fig.4 Crack propagation in tension.

With the same specimen parameters, the uniaxial compressive failure loads are $-25.780\ N/mm^2$, $-16.000\ N/mm^2$, $-15.110\ N/mm^2$ and $-12.500\ N/mm^2$, respectively. The linear regression relation is

$$Log(\sigma) = 5.624 - 0.629 Log(s) \qquad (12)$$

The primitive microcrack distribution with specimen size 100 *mm* in compression is shown in Fig.5(a), whereas the final crack pattern is shown in Fig.5(b). The slope of -0.629 is a little larger than -0.495 in Eq.(11), which means that the size effect in compression is a little more severe compared with the case in tension, but without significant difference.

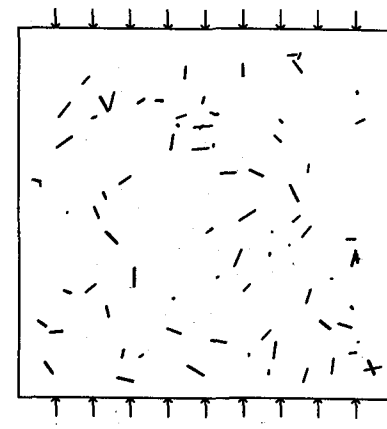

(a) Primitive crack distribution in compression.

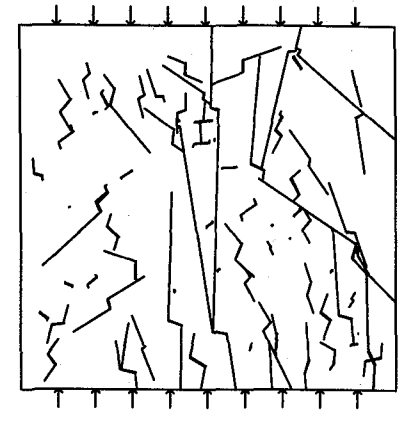

(b) Crack pattern at failure

Fig.5 Specimen in compression.

3.2 Geometrically Similar Specimens in Tension with only one Major Crack

A skew crack of 45^o in tensile mixed mode fracture is computed with DD representation of the cracks. The Young's modulus is assumed as $E=30,000\ N/mm^2$, Poisson ratio $\nu=0.3$, and the Fracture Toughness $K_{IC}=100\ N/mm^{3/2}$. The varied parameters are crack length and the specimen size as shown in detail in Table 1. Typical failure crack pattern is shown in Fig.6, the trajectories of the branching cracks are progressively perpendicular to the major tensile stress. The computed failure stresses are also grouped in Table 1.

From the failure stresses in Table 1, the influences of the crack length, specimen size on the loading capacities of the brittle material in mixed mode fracture can be studied respectively.

Table 1 Specimen Sizes, Crack Lengths and Failure Stresses

Specimen size (*mm*)	400	200	100
Half-crack length (*mm*)	223	111.50	55.75
Failure stress (N/mm^2)	1.6	2.2	3.0
Half-crack length (*mm*)	148.66	74.33	37.16
Failure stress (N/mm^2)	3.2	3.2	6.4
Half-crack length (*mm*)	111.50	55.75	27.87
Failure stress (N/mm^2)	4.8	6.8	9.2
Half-crack length (*mm*)	74.33	37.16	18.58
Failure stress (N/mm^2)	6.8	9.6	13.2

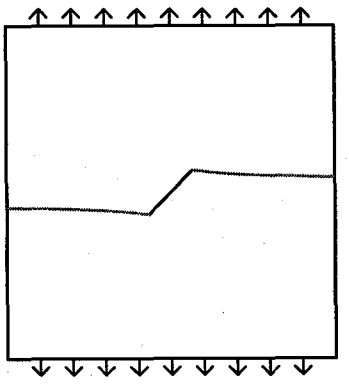

(a) s=400, a=74.33

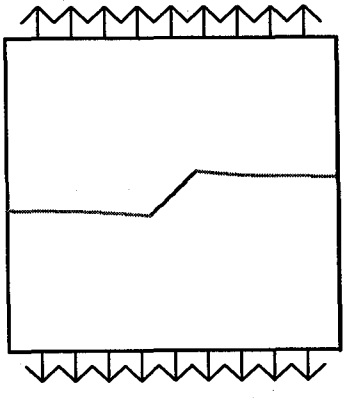

(b) s=200, a=37.14

Fig.6 Typical failure crack patterns in tension.

First, the cases with proportional sizes of crack/specimen (geometrically similar) are checked. When the specimen sizes are taken as 100, 200 and 400 mm, four groups of data are available. The crack/specimen scaling ratios are 0.1858, 0.2787, 0.3716 and 0.5575, respectively. If we make linear regression of the failure stresses and varied specimen sizes in the bilogarithmic form, the following expressions can be obtained:

$$Log(\sigma) = 1.3847 - 0.4534 Log(s) \quad (a/s = 0.5575) \qquad (13a)$$

$$Log(\sigma) = 1.8148 - 0.5000 Log(s) \quad (a/s = 0.3716) \qquad (13b)$$

$$Log(\sigma) = 1.9058 - 0.4693 Log(s) \quad (a/s = 0.2787) \qquad (13c)$$

$$Log(\sigma) = 2.0795 - 0.4785 Log(s) \quad (a/s = 0.1858) \qquad (13d)$$

The variations of the failure stresses with specimen size and crack length in geometrically similar cases are shown in Fig.7. All of the slopes are approximately near the value of -1/2, these values are again just the classical Griffith fracture mechanics stress singularity like the case of in section 3.1.

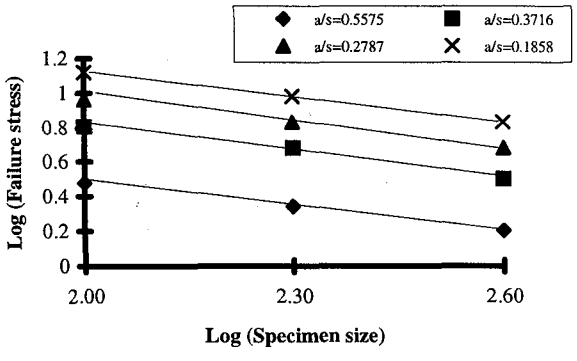

Fig.7 Size effects with geometrical similarity.

3.3 Tensile Crack Length Effects without Geometrical Similarity

When the crack length effect is checked in the case of fixed specimen size with varying crack lengths, as shown in Fig.8, the linear regressive expressions become:

$$Log(\sigma) = 2.8667 - 1.3430 Log(a) \quad (s = 100mm) \qquad (14a)$$

$$Log(\sigma) = 3.1200 - 1.3327 Log(a) \quad (s = 200mm) \qquad (14b)$$

$$Log(\sigma) = 3.3468 - 1.3229 Log(a) \quad (s = 400mm) \qquad (14c)$$

The slopes in above equations are about -1.33, not the -1/2 in the cases of the same crack/specimen ratios. At first glance it seems a little astonishing, however, the result analysis shows that the difference is mainly

attributed to the boundary influences.

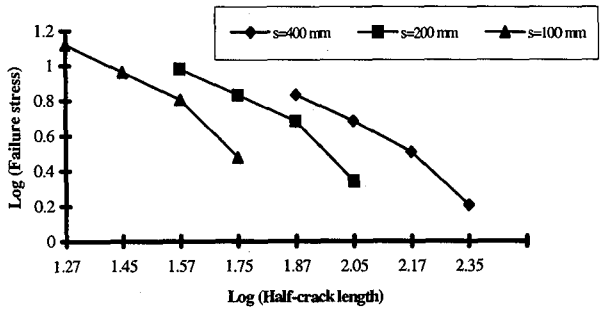

Fig.8 Size effects of crack length with geometrical dissimilarity.

This can be explained with an example by considering the same length of cracks in different sizes of specimens. If the finite sized boundary effects are neglected, the same SIFs at the crack tips will be obtained for the same external stress from the classical fracture mechanics. Therefore, the two different sized specimens with same crack length will have the same failure stress since the unstable crack propagation will occur when the SIFs reach the material fracture toughness. This is obviously not true for practical cases because the boundary far from the crack will exert higher resistance (constraint) on the crack propagation.

In the condition that the two different sized specimens contain the same length of cracks, the larger specimen will have higher strength. The failure stresses of the larger specimens with the same crack lengths are 50% ~ 127% higher than those of smaller specimen sizes, contradicting with the predictions of the same failure strengths from classical fracture mechanics.

So it can be pointed out that the usual Size Effects with -1/2 slope in bilogarithmic form are only applicable to the geometrically similar cases.

3.4 Frictional Compressive Crack without Geometrical Similarity

When the specimen is subjected to compressive stress, the friction on the crack's surfaces is an important factor that affects the strength of the brittle specimen. The friction on the surfaces will exert resistance on the crack propagation in compression. With the same material parameters, the failure stresses of a square specimen of 400 *mm* sides, with varying crack lengths and Coulomb's frictional angles, are computed. Typical failure crack patterns in compression are shown in Fig.9, and the computed failure stresses are grouped in Table 2.

The variations of the failure stresses with different crack lengths are shown in Fig.10. The linear regre-ssions in bilogarithmic form are

$$Log(\sigma) = 4.4425 - 1.6627\,Log(a) \qquad (\varphi = 0^o) \qquad (15a)$$

$$Log(\sigma) = 4.7815 - 1.7624\,Log(a) \qquad (\varphi = 16.6^o) \qquad (15b)$$

$$Log(\sigma) = 4.4754 - 1.5427\,Log(a) \qquad (\varphi = 26.6^o) \qquad (15c)$$

Comparing the slopes in Eqs.(15) and those in Eqs.(14), it can be found that when the crack is in compression, the influence of the crack length on the failure stress is more severe than that with tensile stress.

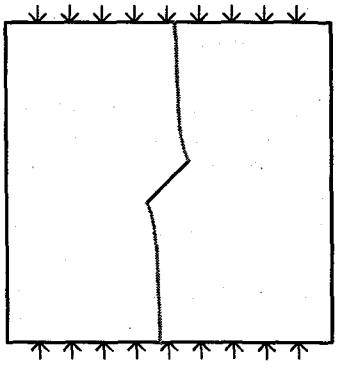

(a) s=400, a=74.33

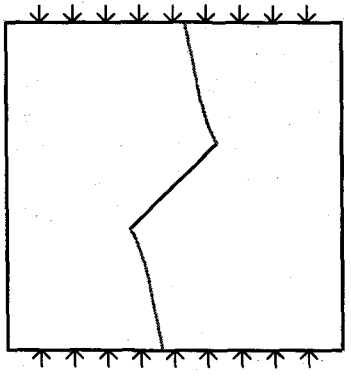

(b) s=400, a=148.66

Fig.9 Typical failure crack patterns in compression.

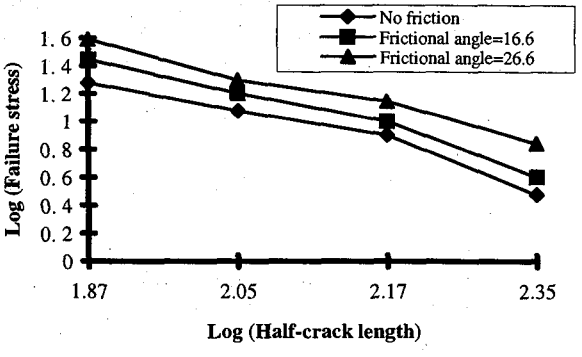

Fig.10 Size effects with different crack lengths in compression.

Table 2. Failure Stresses with Varied Crack Lengths and Frictions
(Failure stresses in N/mm^2, specimen size $s= 400\ mm$)

Half-crack lengths (*mm*)	74.33	111.50	148.66	223.00
No friction	-19	-12	-8	-3
Frictional angle 16.6°	-28	-16	-10	-4
Frictional angle 25.6°	-39	-20	-14	-7

4. Concluding Remarks

To understand the crack-sensitive failure mechanism of brittle materials, the crack propagation processes of the finite sized specimens are simulated with the help of two micromechanics models. The coefficients representing coupling between cracks and finite sized boundary are obtained in the form of algebraic expressions, and the curved propagating trajectories or simplified straight branching paths are simulated through a stepwise incremental process.

With geometrical similarity and dissimilarity, the influences of crack length and specimen size on the strength of brittle materials in both tension and frictional compression are studied. It is found that in the cases of geometrically similar specimens (with same crack to specimen ratios), the failure stresses decrease with the increase of the specimen size (or crack length) by a slope of -1/2 in the bilogarithmic form. However, in cases of geometrical dissimilarity, the size effects present different features: usually they are more severe than those of geometrically similar cases. It is therefore verified that the usual Size Effect Laws connected with the slope -1/2 are only applicable to the geometrically similar cases.

Since the geometrical similarity does not always hold for the practical engineering cases, the applications of the previous Size Effect Laws should be further studied considering the real engineering situations.

Acknowledgment

The kind helps of Prof. A. Carpinteri and Prof. C. Scavia of politecnico di Torino are gratefully appreciated, and the Fellowship from the Japan Society for the Promotion of Science is also greatly acknowledged.

References

1. Z.P. Bazant, Size effect in blunt fracture: concrete, rock, metal, *J. of Engng. Mechanics*, ASCE, **110**, 518-535, 1984.
2. A. Carpinteri, (Ed.), *Applications of Fracture Mechanics to Reinforced Concrete*, Elsevier Applied Science, London and New York,1992.
3. S. P. Shah, S. E. Swartz and C. Ouyang, *Fracture Mechanics of Concrete*, John Wiley & Sons, Inc, 1995.
4. J. Bolander Jr. and H. Hikosaka, Simulation of fracture in cement-based composites, *Cement & Concrete Composites*, **17**, 135-145, 1995.
5. Y. V. Zaitsev and F. H. Wittmann, Simulation of crack propagation and failure of concrete, *Materials and Structures*, **14**, No.83, 357-365, 1981.
6. H. Horii and S. Nemat-Nasser, Brittle failure in compression: spliting, faulting and brittle-ductile transition, *Phil. Trans. R. Soc. London*, **A 319**, 337-374, 1986.
7. M. Kachanov, Elastic solids with many cracks: a simple method of analysis, *Int. J. of Solid and Struct.*, **23**, No.1, 23-43, 1987.
8. Guo-ping Yang and Xila Liu, Interaction and propagation of random microcracks in compression, *Studi e Ricerche, Italy*, **14**, 121-141, 1993.
9. S.L. Crouch and A.M. Starfield, *Boundary Element Methods in Solid Mechanics*, George Allen and Unwin, London, 1983.
10. I.N. Sneddon and M. Lowengrub, *Crack Problems in the Classical Theory of Elasticity*, John Wiley & Sons Inc., 1969.
11. A. Carpinteri and Guo-ping Yang, Fractal dimension evolution of microcrack net in disordered materials, *Theoretical and Applied Fracture Mechanics*, **25**, No.1, 73-81,1996.
12. A. Carpinteri, C. Scavia and Guo-ping Yang, Microcrack propagation, coalescence and size effects in compression, *Engineering Fracture Mechanics*, **54**, No.3, 335-347, 1996.
13. C. Scavia, A method for the study of crack propagation in rock structures, *Geotecnique*, **45**, 447-463, 1995.
14. A. Carpinteri and Guo-ping Yang, Size Effects in Brittle Specimen with Microcrack Interaction, *Computers & Structures*, 1996(in press).

(Received September 6, 1996)